The Cutting Edge – Micro-CT for Quantitative Toolmark Analysis of Sharp Force Trauma to Bone

HIGHLIGHTS

- Micro-CT was demonstrated to be a valuable toolmark analysis and visualization tool
- Quantitative knife toolmark properties can be easily extracted from micro-CT data
- Mechanically made toolmarks differ from those made under more real-world conditions
- Serrated and plain blades produce statistically different toolmark properties
- Toolmarks correlate with knife properties allowing successful predictive modelling

ABSTRACT

Toolmark analysis involves examining marks created on an object to identify the likely tool responsible for creating those marks (e.g., a knife). Although a potentially powerful forensic tool, knife mark analysis is still in its infancy and the validation of imaging techniques as well as quantitative approaches is ongoing. This study builds on previous work by simulating real-world stabbings experimentally and statistically exploring quantitative toolmark properties, such as cut mark angle captured by micro-CT imaging, to predict the knife responsible. In experiment 1 a mechanical stab rig and two knives were used to create 14 knife cut marks on dry pig ribs. The toolmarks were laser and micro-CT scanned to allow for quantitative measurements of numerous toolmark properties. The findings from experiment 1 demonstrated that both knives produced statistically different cut mark widths, wall angle and shapes. Experiment 2 examined knife marks created on fleshed pig torsos with conditions designed to better simulate real-world stabbings. Eight knives were used to generate 64 incision cut marks that were also micro-CT scanned. Statistical exploration of these cut marks suggested that knife type, serrated or plain, can be predicted from cut mark width and wall angle. Preliminary results suggest that knives type can be predicted from cut mark width, and that knife edge thickness correlates with cut mark width. An additional 16 cut marks walls were imaged for striation marks using Scanning Electron Microscopy with results suggesting that this approach might not be useful for knife mark analysis. Results also indicated that observer judgements of cut mark shape were more consistent when rated from micro-CT images than light microscopy images. The potential to combine micro-CT data, medical grade CT data and photographs to develop highly realistic virtual models for visualisation and 3D printing is also demonstrated. This is the first study to statistically explore simulated real-world knife marks imaged by micro-CT to demonstrate the potential of quantitative approaches in knife mark analysis. Findings and methods presented in this study are relevant to both forensic toolmark researchers as well as practitioners. Limitations of the experimental methodologies and imaging techniques are discussed, and further work is recommended.

Keywords

Micro-CT
Toolmark analysis
Cut marks
Knife / Knives
Scanning electron microscopy (SEM)
Striations

1.0 INTRODUCTION

The most common method of murder in the UK is through the use of sharp instruments such as knives [1,2]. Forensic pathologist typically conduct toolmark analysis to determine the type of instrument and level of force used, the trajectory of the weapon during impact, and the position of the victim and perpetrator during the assault [3]. No tool type produces exactly the same toolmark, which makes analysis of the remaining marks a powerful forensic method. [4]. Toolmark Analysis of Sharp Force Trauma covers a broad range of tools [5] including saw marks [6-10] and hacking marks [11-13], typically found in body dismemberment, and knife marks [13-21] seen in fatal stabbings – the will be examined in this study.

In knife mark analysis experiments the simulation of real-world stabbings is difficult and therefore it is not surprising that previous work have started with tightly controlled experimental produces. These often use defleshed or dry bone samples which are clamped whilst toolmarks are made by either the experimenters [17-19] or by some mechanical means [15,20-21]. However, knife type distinctions are more difficult when toolmarks are made in real-world conditions when factors such as tissue presence, bone elasticity [22], knife impact and knife trajectory are more variable. Indeed, using more realistic conditions Ferllini (2012) demonstrated, contrary to previous consensus, it was not possible to determine knife type from the toolmarks due to significant variability in their properties [23]. This is concerning as toolmark analysis has come under legal scrutiny in recent years, via the Daubert Standards introduced by the US Supreme Court [24] and Section 20 of the UK Forensic Science Regulator's Code of Practice.

Traditional light microscopy has been the primary imaging method for toolmark analysis [25, 26-27]. However, although possible [28] determining quantitative toolmark properties with this method can be unreliable [29]. Furthermore, without destructive methods, toolmark information that is not visible from the surface, such as wall angle and depth, cannot be obtained [30]. Fortunately, alternative methods are being developed. Scanning Electron Microscopy (SEM) has been used to measure knife mark widths [31, 20], and is currently unique in being able to reveal striation patterns imprinted on cut mark walls which are strongly diagnostic for determining saw type [21]. Numerous studies aimed at identifying knife striations in costal cartilage have produced mixed results [21, 23, 31-35] and the authors know of no studies investigating knife striations in bone. Optical laser scanning can capture 3-dimensional (3D) data at a resolution around 100µm+ [36]. This has been used for; crime scene scanning [37], traffic accident documentation [38], blunt force injury capture [39-41], and model creation for 3D printing [42-43]. Sansoni et al (2009) provided initial support that laser scanning could also be used in knife and saw marks analysis [36]. Crucially though none of the above methods allow for the internal toolmark properties to be captured non-destructively [44-45]. Although Medical grade CT has been shown to be an effective method for identifying the presence of toolmarks in-situ, [46-47] its relatively poor spatial

resolutions (>300µm) precludes it as an alternative to microscopy for extracting toolmark properties [28, 30, 48]. However, micro-CT is likely to be more appropriate for the extraction of toolmarks properties due to its significantly higher spatial resolution (0.5-100µm) [14].

The application of micro-CT in forensic investigations has been pioneered by Thali et al [14], Rutty et al [48] and others, applying it directly to toolmark analysis [9, 17, 47, 49-50]. Thali et al created puncture marks in pork shoulders and using micro-CT took 2D slices of the puncture marks before visually overlaying the knife blade tip to suggest a match [14]. Rutty et al described and demonstrated, with a small sample of different bone traumas, the potential of micro-CT for forensic science [48]. Capuani et al's study however suggested that micro-CT could not be used to distinguish between knife marks, however it was noted that their sample size was small [17]. Gaudio et al used cone beam CT to image puncture marks on bone at a relatively low resolution of 100-300µm^3 before exporting the data as 3D mesh models to Geomagic Studio where measurements of the length, depth and width were taken [50]. The errors in measuring the toolmark geometries were ±0.6mm with the author describing the 3D reconstructions as *"extremely realistic 3D models"* – the present authors suggest that this can be much greater with current technology. Furthermore, micro-CT has also been recommended as an effective method for saw mark analysis [9]. A recent study by Pelletti et al showed that micro-CT allowed for clear objective measurements of saw marks with high agreement across different raters [10]. Baier et al, showed how micro-CT could be used successfully in a homicide case and, although no formal toolmark analysis was performed, the authors noted that micro-CT did allow for excellent visualisation of toolmark properties [44]. Finally, other non-sharp force trauma toolmark studies, such as those by Giraudo et al, have demonstrate micro-CT as a useful tool for gunshot residue analysis [51]. Although these few studies show great potential for micro-CT as a non-destructive toolmark imaging technology, the previous studies contained only a small number of cut marks with little to no quantitative toolmark analysis conducted. Asides from quantitative methods, micro-CT has other benefits in toolmark analysis. For example, it allows the possibility of creating high resolution 3D models that can be fused with medical CT scans – such as placing a toolmarked rib its anatomical context. Photographs of the defleshed toolmarks can be mapped onto the fused model providing additional colour information such as bone staining. Susepcted knives and these 3D models could be imported into the 3D digital environment allowing digital attempts of weapon-wound matching. These 3D models could be printed and used as visual props for forensic investigators or a jury [42-43].

In summary, the current study aims to evaluate a range of toolmark analysis imaging methods and 3D visualisation techniques and determine whether these methods can identify toolmark properties that allow for the statistical determination of knife type from knife marks created on bone as a result of a simulated stabbing incident.

2.0 MATERIALS AND METHODS

2.1 Methodology Summary

Given the complexity of the methodology i.e. two experiments, various imaging methods assessed, and different analyses preformed, a diagrammatic summary of the methodology is presented [Fig.1.].

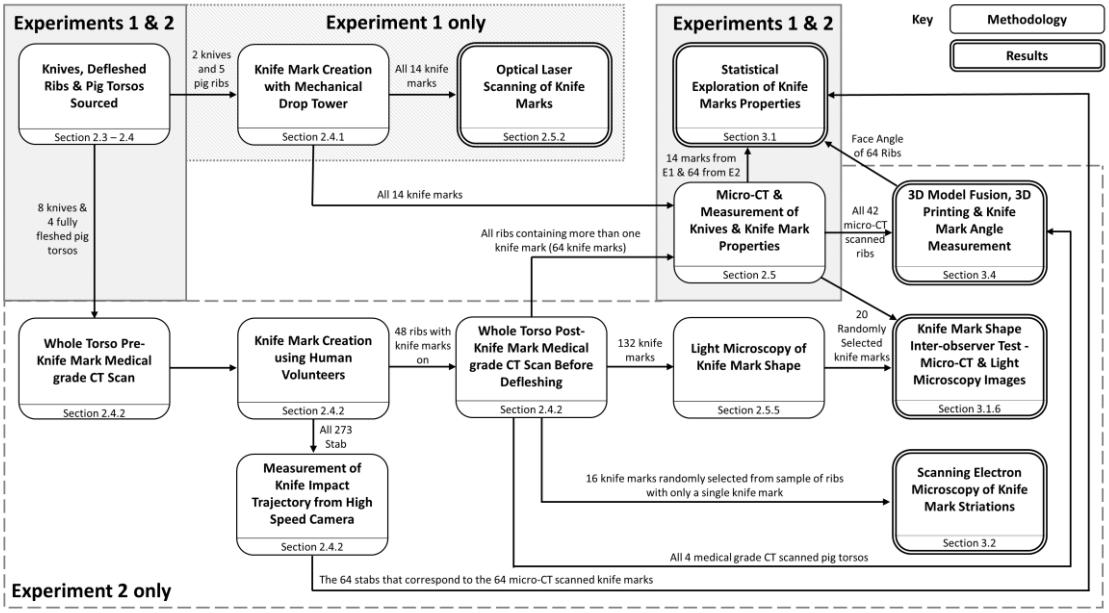

Fig. 1. *Diagrammatic summary of the study including experiment 1 and 2, each different imaging method and analysis and which section of the article to reference*

2.2 Terminology

Toolmarks resulting from sharp instruments such as knifes are often called cut marks and can be classified into clefts, punctures or incisions [5]. Previous work has already demonstrated how micro-CT could be used to analyse puncture marks [14], therefore the focus of this study is incision cut marks. Given the lack of standardisation in the literature regarding toolmark terminology, specific definitions are provided [Fig. 2.].

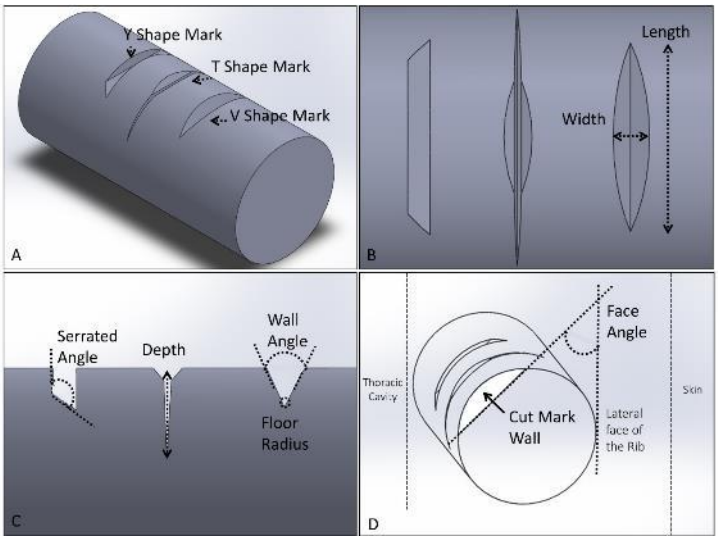

Fig. 2. *Cut mark terminology A) 3D model examples of cut mark shapes, Y, T and V, usually made by different knife types B) The width is defined as the minimum distance between the edges of the cut mark and is measured at the surface of the bone thereby does not include cut mark wastage. Cut mark length is the minimum distance between the start and end of the cut mark. C) The wall angle is the maximum angle between the two adjacent walls intersecting on the cut mark floor. The serrated angle, only present in Y shaped cuts marks, is the maximum (obtuse) angle between the wall that does not intersect the floor and its adjacent wall which does. The depth is the maximum distance from the cut mark floor to the surface of the bone. The floor radius is the radius of the circle whose perimeter in tangential to the two adjacent walls intersecting on the cut mark floor. D) The measurement of face angle is described as the angle between the lateral face of the rib (i.e. the face of the rib facing away from the body) and the cut mark floor. Striations are observed on the wall of the incision mark highlighted white. Note that some of these measures (serrated angle, face angle and floor radius) have not been described in previous literature, possibly because they would be difficult to visualise without the use of micro-CT.*

2.3 Knives Sourced

Five confiscated worn knives from the Physical Protection Group of the Metropolitan Police (knives 1-2 and 6-8, [Fig. 4.]) with an additional 3 worn kitchen knives (knives 3, 5 & 9, [Fig. 4.]). One serrated (knife 4) and one plain knife (knife 5) were used in Experiment 1 and four serrated and four plain knives were used for Experiment 2 (knife 4 was used in both experiments). Quantitative measures of the knife properties [Fig. 5.] as recommended by Ferrilli (2012) [23], are presented [Table. 1].

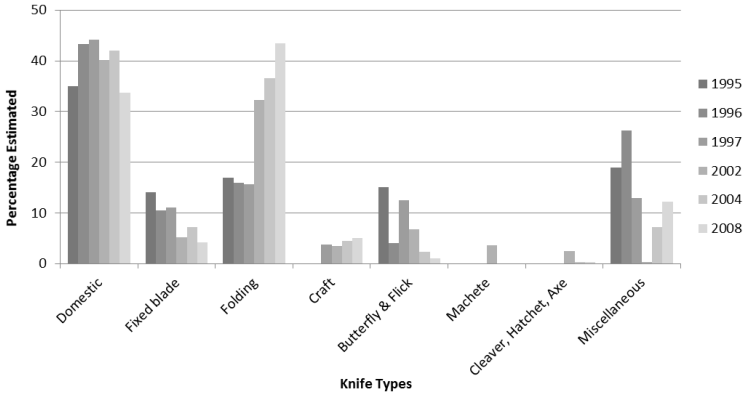

Fig. 3. *Classes of knives that are either confiscated from prisoner's property or confiscated from the street between 1995 and 2008 by the Physical Protection Group of the Metropolitan Police [52].*

Table 1

Properties of knives used in Experiments 1 and 2

Key	Knife Type	Individual Knife	Tip Angle (°)	Edge Angle (°)	Serrated angle (°)	Edge Thickness (mm)
1	Serrated	Steak[1]	45	23	164	0.86
2	Serrated	Fishing[2]	60	34	158	0.77
3	Serrated	Pairing[2]	42	37	146	0.61
4	Serrated	Steak[2]	49	50	140	1.03
5*	Plain	Vegetable[4]	50	42	n/a	0.88
6	Plain	Folding[4]	57	29	n/a	0.42
7	Plain	Cook's[3]	70	44	n/a	0.33
8	Plain	Cleaner[3]	34	35	n/a	0.67
9	Plain	Carving[4]	75	23	n/a	0.31

[1] Double serration [2] Classic serrations [3] Flat bevel [4] Asymmetrical flat bevel *Only used in Experiment 1

Fig. 4. *From left to right, Knives 1-4 serrated, 5-9 plain edged. Five Confiscated knives donated by the Physical Protection Group of the Metropolitan Police (Knives 1-2 & 6-8), and two knives (Knives 3 & 9) used in experiment 2. One knife (Knife 5) used solely in experiment 1 along with Knife 5.*

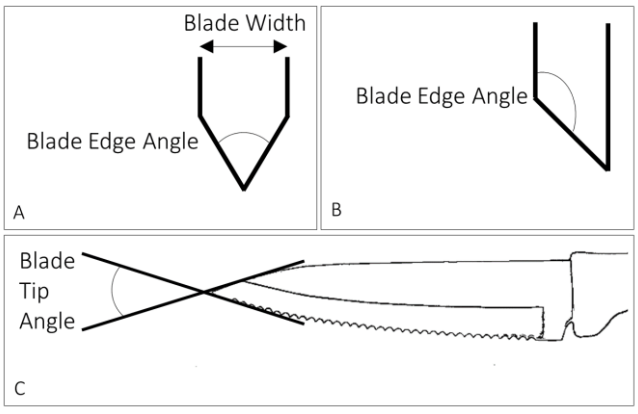

Fig. 5. *Diagram of knife properties reported in Table 1. A) A Plain blade grind cross section showing the Blade Edge Thickness, the thickness of the blade at the top of the cutting edge, and the Blade Edge Angle relating to the sharpness of the cutting edge; B) A Serrated blade grind cross section showing the Blade Serrated Angle, similar to the serrated angle for cut marks but is only present on serrated blades, is the maximum (obtuse) angle between the blade face not intersecting the cutting edge and the adjacent cutting face and C) Blade profile showing the Blade Tip Angle relating to the point of the tip*

2.4 Knife Mark Procedures

2.4.1 Experiment 1 Procedure

To understand conflicting findings in the literature, one aim was to compare toolmarks made in a more controlled manner (Experiment 1) against those made in a more simulated real-world fashion (Experiment 2). Cut marks were created on dry bone using mechanical means [15, 17-18, 21, 35, 46]. To replicate a "push and thrust" effect seen in human stabbing kinematics [53], a Home Office Body Armour Drop Test Rig [Fig. 6A.] consisting of a 1.9kg missile with plastozote dampers was used. Knife impact energy was specified as 45J typically delivered in a human knife attack [54]. Three pig ribs were sourced from a butcher, manually defleshed, and air dried prior to testing [18, 20, 15-26]. The ribs were placed on a standard clay backing with approximately ¼ of the rib edge in the path of the knife projectile [Fig. 6B.]. 7 marks were generated each by two knives (knives 4 and 5, [Fig. 6C.]) generating 14 incisions for imaging [Fig. 6D.].

Fig. 6. *A) Drop Test Rig; B) Knife marking dry rib; C) Two knives used in experiment 1, Knife 4, left and Knife 5 right; and D) 4 cut marks generated by Knife 4*

2.4.2 Experiment 2 Procedure

In contrast to Experiment 1, Experiment 2 aimed to create more realistic toolmarks. Due to their similarities to human tissue [18, 23, 55] and as the torso is the most targeted region during knife attacks [18, 23, 35] four fully fleshed pig (*sus scrofa*) torsos were sourced from a medical meat supplier. For practical reasons such as storage and medical imaging, the organs were replaced with tightly compacted High-Density Polyethylene bags and the samples were then stitched up to mimic typical skin tension. High-Density Polyethylene is similar in density to human tissue and would therefore partially simulate blade resistance. To mimic human skin thickness, subcutaneous fat was thinned and to create clothing resistance, white T-shirts were then stitched on the torsos [23] which also allowed labelling of the individual stab wounds with a fabric pen. As a pre-experiment baseline, the whole samples were scanned using a GE 'Medical' grade CT system (resolution 300µm) before being refrigerated overnight. Rather than rigidly holding the torsos in position, the samples were placed upright so that the torso was approximately the anatomical height of an average male torso and then rested against a 5cm solid thick polystyrene sheet which was supported by a clamp. This allowed the sample to partially recoil on impact to simulate the non-rigid recoil of a human victim [23]. Lightly held at each side to reduce lateral

movement [Fig. 7.] the samples were mounted with one side of the ribs perpendicular to the human volunteer ensuring knife to rib contact. A Casio EX-ZR100 camera recorded each knife impact at 240fps with video software used to measure the knife impact trajectory relative to the surface of the sample (serrated knife trajectory was later used for analysis).

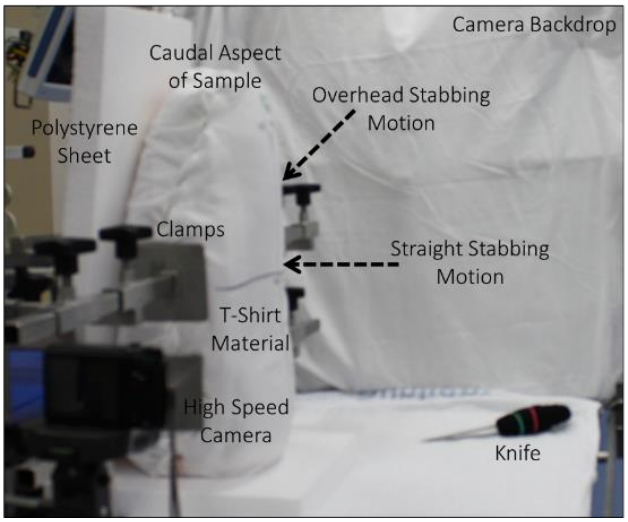

Fig. 7. *Pig torso sample with white material outer layer clamped in an upright orientation positioned at average torso height prior to cut mark generation by human effort.*

Two right handed male volunteers performed underarm and overhead stabs with moderate force, anywhere on the sample between ribs 4-10, thereby not restricting the volunteers to adopt an unnaturally precise action. 10 stabs per volunteer per stab type and per knife was planned, equating to 320 stabs. However, two of the serrated knives broke (Knife 1 snapped midway along the blade after 7 impacts and Knife 2 snapped at the handle after 26 impacts) leading to 273 stabs in total. The volunteers noted that the serrated blades allowed for a much more *"penetrating"* and *"controlled"* stabbing and that wider knives didn't penetrate very far often stopping with just the tip perforating the skin presumably due to the intercostal rib spaces. Samples were scanned again using medical grade CT (resolution 300µm) with the tissue cut marks now clearly visible from the scans [Fig. 8.]. This provided baseline scans of the ribs in their anatomical positions, allowing for subsequent model fusion with the micro-CT data. Following medical CT scanning the pig samples were stored overnight in a fridge.

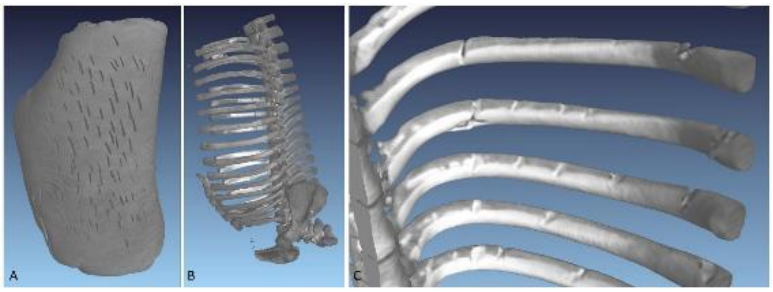

Fig. 8. *A) Medical grade CT scan of the tissue B) bone from a pig torso and C) cut marks sample following human stab cut mark generation conducted in experiment 2.*

The ribs were manually dissected out by a trained anatomist, ensuring no confounding cut marks were created. A mechanical saw separated the ribs at the spine ends and a surgical knife cut between the intercostal spaces to separate each individual rib. It was noted that the ribs stabbed with Knife 3 were shattered, and although a single rib was salvaged, the rest were discarded. Defleshing and preparing the rib samples was done using a chemical antiformin solution method proposed by Snyder et al [56] (for alternative methods including burying, water maceration, mechanical removal, boiling, biological detergent, bleach, use of dermestid beetles and chemical solutions, see [57-65]). The antiformin solution was prepared by mixing 150g of sodium carbonate with 250mL water and 100g of calcium hypochlorite with 750mL water. These solutions are then combined to form a 1L sodium carbonate – calcium hypochlorite solution and then continually stirred over the course of 3-4 hours. 150g of sodium hydroxide was added to 1L of water before combining with sodium carbonate to create a concentrated calcium hypochlorite solution. The antiformin solution diluted 1:8 with water was slowly heated to approximately 85°C and the rib samples placed in for approximately 3 minutes with constant monitoring. The samples were then removed and rinsed thoroughly in warm water removing any remaining soft tissue with a sponge. Degreasing was done by simmering the samples in a 50% ammonia solution for approximately 4 hours. They were then left to air dry for 24 hours before being placed in a 1-3% hydrogen peroxide solution for approximately 1 hour to allow slight whitening and preservation. The samples were left to air dry for 2-3 days and the labels were replaced with ink labels written on the bone surface. An example of two ribs defleshed with the toolmarks produced by Knife 4 [Fig. 9A.] and 8 [Fig. 9B]. is shown below. Four samples were damaged due to experimenter error in the form of prolonged exposure to the antiformin solution and were therefore removed from further analysis. The 42-remaining ribs contained 132 cuts marks of varying types.

Fig. 9. *Defleshed pig rib from experiment 2 with A) 7 cut marks made by knife 4; and B) 3 marks made by knife 8*

2.5 Imaging

2.5.1 Micro-CT Imaging

Using a Nikon XT H 320LC Micro-CT scanner, each rib was scanned individually with resolutions between 10-30µm. Scanning parameters were 90kV, 6W, 2 second exposure, no filter and 6-14 magnification resulting in scan times around 3 hours per rib. The data were reconstructed using Nikon's Proprietary software, *CT Pro* and then exported to VGStudio Max for toolmark measurements [Fig. 10.] using the same process documented in Thornby et al [66]. The toolmark properties [Fig. 2.] were then measured in VGStudio Max.

All 14 incisions from Experiment 1 were scanned. In experiment 2, cleft (15 marks) and puncture (19 marks) marks were filtered out prior to imaging. As micro-CT scanning is time consuming (approximately 3 hours per scan) and expensive, an a-prior decision was made to only scan ribs containing 2 or more toolmarks. The total number of marks micro-CT scanned in experiment 2 was 64, with 33 created by serrated knives and 31 by plain knives. The number of cut marks micro-CT scanned at the individual knife level was; 0, 3, 7, 23, 8, 11, 8, 4 for Knives 1-9 respectively. In total, 64 incisions were scanned in Experiment 2. Each knife blade was also scanned (parameters 225kV, 17W, 1.4 second exposure, 1mm copper filter and 1-10 magnification) before being reconstructed and exported as surface files.

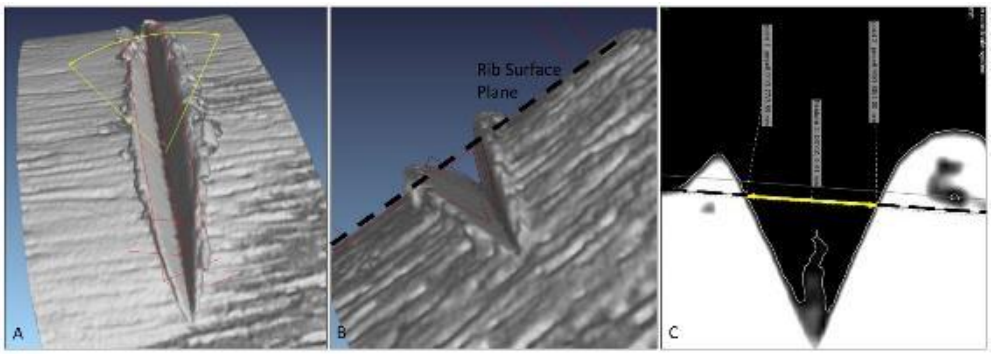

Fig. 10. *Example of virtual measurement of cut mark micromorphological on V shaped micro-CT scanned cut mark. A) Wall angle measurement; B) Width measurements; C) 2D view cross section of width measurement*

2.5.2 Optical Laser Scanning

Following pilot work by Sansoni et al (2009) [36], we assessed the effectiveness of optical laser scanning for toolmark analysis. A Nikon K6 10 Series manual measurement arm was used to scan all 14 cut marks from Experiment 1. The ribs were lightly clamped and scanned at approximately 120µm, creating point cloud data that was exported to Geomagic Studio as 3D polygon data. However, it was difficult to capture the visible cut mark interior and often resulted in incomplete mesh surface data unsuitable for further analysis. No additional analysis or laser scanning was performed.

2.5.3 Scanning Electron Microscopy

Eight serrated cut marks and eight plain cut marks were randomly selected from ribs that were filtered out from micro-CT scanning due to only having a single cut mark per rib. To separate cut mark walls, the ribs were carefully sawn from the underside of the cut mark to the cut mark floor. One was completely sawn through and SEM imaged providing baseline saw striations [23]. Following the separation of the walls, samples were cut to size, fixed to metal studs with a silver paint, gold sputtered and then imaged in a Sigma SEM machine (lateral spatial resolutions ≈3µm).

2.5.5 Light Microscopy

Consistent qualitative assessment of knife toolmark across forensic practitioners is desired when categorising toolmark shape. The levels of agreement, measured as inter-observer reliability, between 10 participants for the categorisation of toolmark shape was compared between micro-CT and light microscopy. A Nikon SMZ 745T microscope, captured images of the cut marks in experiment 2 to compare cut mark shape classification objectivity with micro-CT images. 10 participants (aged 18-43, 4 females) from the university with no prior knowledge of toolmark analysis classified images of cut mark shapes based on micro-CT cross-sections images and microscope images [Fig. 11.]. Participants completed a questionnaire which included examples of pre-classified cut mark shapes as training before judging 20 paired microscope and micro-CT cut marks shapes, presented in a random order, as either 'V', 'Y', 'T', 'neither' or 'unsure'. Interobserver agreement was assessed using; Fliess's Kappa, Krippendorff's alpha and average pairwise % agreement. Criteria for 'good' agreement in each test is 0.7+, 0.6+ and 75%+ respectively [67-72].

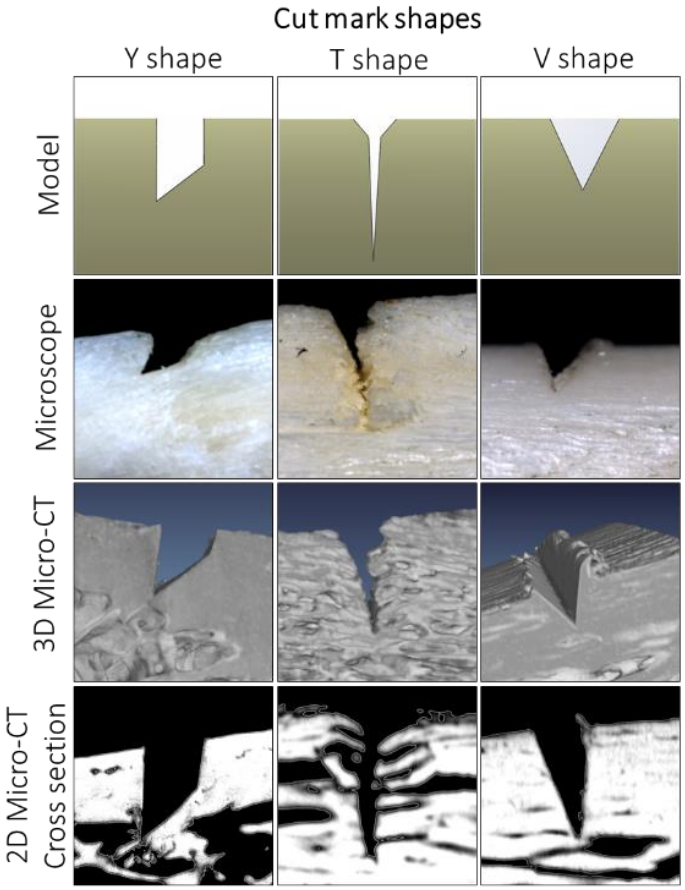

Fig. 11. *Example cut mark shapes Y, T and V presented as idealised model, microscope image, 3D micro-CT image and 2D micro-CT cross section. Images like the ones above were given separately to participants to classify the cut mark shape as either V, T, Y, 'neither' or 'unsure'*

2.5.6 Model Fusion and Visualisation

Medical grade CT, micro-CT, laser scanning and photographs from experiment 2 were used to develop 3D models that facilitated data storage and processing, visualisation, 3D printing and virtual analysis. The Medical CT 3D data provided relatively low resolution models (300µm) providing anatomical context for individual micro-CT scanned models. High resolution micro-CT surface data of bone was extracted using the method described by Norman et al (2014) and was used to combine the micro-CT and medical CT data [73-74]. Key regions of interest e.g. cut marks or the acutal knife blades, were kept at full resolution (≈30µm) whilst contextual information was reduced in fidelity enabling file size reduction from approximately 40GB to approximately 40Mb. This stage is crucial to allow fusion of all the micro-CT scanned ribs with the medical CT scanned torso as without it the file size would be too great to handle in Geomagic Studio (a 3D mesh software) with currently available systems. The knife blade scans were imported in Geomagic Studio in as free floating models. Digitial photos of the ribs and knives were taken to capture all avaliable surface detail. These photos were mapped onto the micro-CT rib models using 'Texture Mapping' in Geomagic Studio producing high resolution coloured surface models that facilitated data storage/processing, visualisation, 3D printing and virtual analysis. Finally, these 3D models were 3D printed with a resolution of 40µm using a Fortus 400mc Printer

3.0 RESULTS

3.1 Toolmark Analysis

3.1.1 Knife type differences

In Experiment 1, 14 toolmarks were mechanically created on dry pig bone using one serrated and one plain edged blade. The authors noted that quantitively and quantitatively these mechanically made toolmarks were very uniform and clean [Fig. 12.]. In experiment 2, 64 incision marks were micro-CT scanned for analysis and these were notably more variable both within and between individual knives [Fig. 13.].

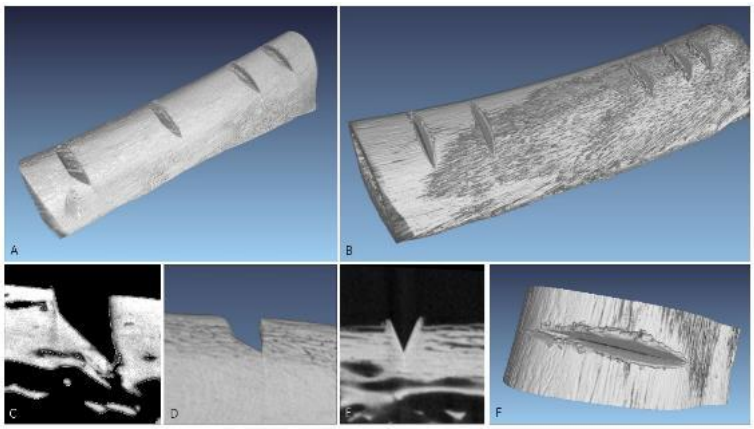

Fig. 12. *Experiment 1 Micro-CT image of: A) Four cut marks from a serrated Knife, (knife 4); B) Five cut marks from by a plain Knife (knife 5); C) 2D cross section of ideal Y shaped cut mark from serrated Knife; D) 3D Y shaped cut mark from serrated blade; E) 2D cross section of ideal V shaped cut mark from a plain blade and F) 3D top down view of cut mark from a plain knife*

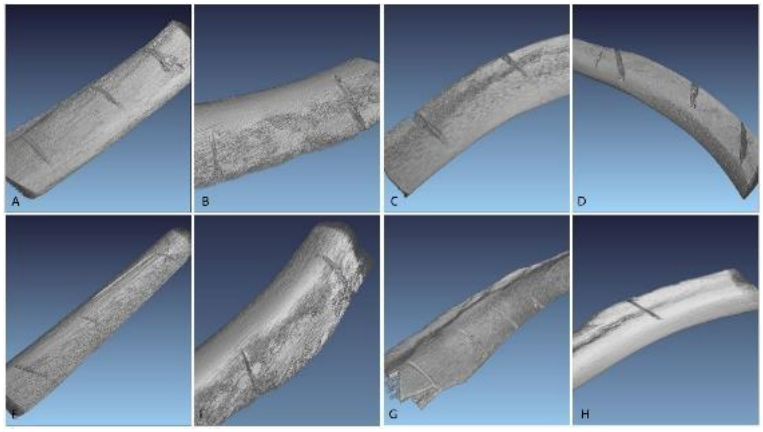

Fig. 13. *Experiment 2 Micro-CT images of: A) Three cut marks made by Knife 1; B) Two cut marks made by Knife 2; C) Two cut marks made by Knife 3; D) Four cut marks made by Knife 4; E) Four cut marks made by Knife 6; F) Two cut marks made by Knife 7; G) Four cut marks made by Knife 8; H) A cut mark made by Knife 9.*

To assess whether the two knife types in this study produced significantly different toolmarks, two one-way multivariate analyses were conducted using the toolmark properties measured from the micro-CT for both experiment 1 [Table 2] and experiment 2 [Table 3]. The one-way multivariate analysis results from experiment 1 and 2 suggest that in our sample of knives, the serrated blades produced significantly different cut mark micro-morphologies compared to the plain / non-serrated blades. A boxplot of the cut mark properties from

278 Experiment 2 is also provided to illustrate these the differences [Fig. 14.]. For the purpose of statistical analysis,
279 we considered each cut mark to be independent any other cut mark irrespective of knife, volunteer, stab
280 trajectory and pig torso.
281
282 Finally, we determined whether the generated cut mark shapes could be used to discriminate between serrated
283 and plain knives. The shape of all cut marks were classified as either 'Y', 'T', 'V' or 'unsure' [Fig. 2.] by the first
284 author and compared with the identity of the knife that produced them. In Experiment 1 all knife marks
285 categorised as Y shaped were generated from by the serrated knives and all those categorised as V shaped were
286 generated by plain knives. In experiment 2, 94% of V shaped cut marks were made by plain blades, 100% of Y
287 shaped cut marks were created by serrated blades and T cut mark shapes were shared by 54% of plain blades
288 and 46% of serrated blades.
289

Table. 2.

Experiment 1: Mean Toolmark properties for blade type (Data are expressed as mean ± standard deviation) and one-way multivariate ANOVA results. Independent variable was blade type (Serrated or Plain) and dependant variable were the toolmark properties (Width, Wall angle and Floor Radii). Combine dependants: $F(3,10)=19.134$, $p<0.001$

Cut Mark Properties	Serrated Blade	Plain Blade	Statistical Results
Width (mm)	1.07 ± 0.33	0.64 ± 0.14	$F(1,12)=62.48$, $p<0.001$
Wall angle (°)	42.1 ± 2.8	50.1 ± 6.7	$F(1,12)=8.62$, $p<0.05$
Floor radii (mm)	0.034 ± 0.005	0.031 ± 0.16	$F(1,12)=0.21$, $p=0.66$

Assumptions: There were no univariate outliers in the data, as assessed by inspection of boxplots. Preliminary assumption checking revealed that the data were not normally distributed, as indicated by Shapiro-Wilk test, there were no univariate or multivariate outliers, as assessed by boxplot and Mahalanobis distance, respectively; there were linear relationships (except for floor radius), as assessed by scatterplot, no multicollinearity; and there was homogeneity of variance-covariance matrices, as assessed by Box's M test. Given that the one-way MANOVA is fairly robust to deviations from normality no corrections were performed. There was homogeneity of variance-covariances matrices, as assessed by Box's test of equality of covariance matrices.

Table. 3.

Experiment 2: Mean Toolmark properties for blade type (Data are expressed as mean ± standard deviation) and one-way multivariate ANOVA results. Independent variable was blade type (Serrated or Plain) and dependant variable were the toolmark properties (Width, Wall angle and Floor Radii). Combine dependants: $F(3,60)=33.5$, $p<0.001$

Cut Mark Properties	Serrated Blade	Plain Blade	Statistical Results
Width (mm)	1.1 ± 0.28	0.54 ± 0.26	$F(1,62)=73.1$, $p<0.001$
Wall angle (°)	47.3 ± 12.4	23.1 ± 13.0	$F(1,62)=57.9$, $p<0.001$
Floor radii (mm)	0.07 ± 0.033	0.035 ± 0.18	$F(1,62)=30.0$, $p<0.001$

Assumptions: There were no univariate outliers in the data, as assessed by inspection of a boxplot. Preliminary assumption checking revealed that data were marginally non-normally distributed, as assessed by the Shapiro-Wilk test, there were no univariate or multivariate outliers, as assessed by boxplot and Mahalanobis distance, respectively; there were linear relationships, as assessed by scatterplot, no multicollinearity; and there was homogeneity of variance-covariance matrices, as assessed by Box's M test. Given that the one-way MANOVA is fairly robust to deviations from normality no corrections were performed. For width and wall angle there was homogeneity of variance-covariances matrices, as assessed by Box's test of equality of covariance matrices but not for floor radius.

290

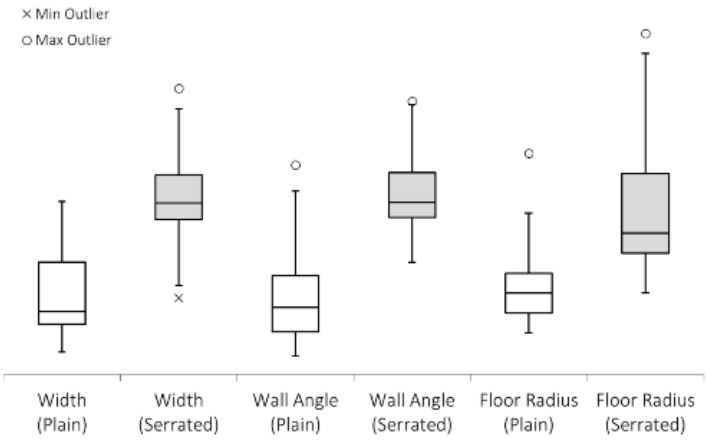

Fig. 14. *Normalised boxplots of cut mark micro-morphology (width, wall angle and floor radius) for knife types plain and serrated (serrated in grey) measured in Experiment 2.*

3.1.2 Knife Prediction

A Binomial Logistic Regression was conducted to determine the predictive value of combining toolmark properties to classify knife type, serrated or plain. The model accounted for 78% of the variance in knife type and correctly classified 94% of cases of toolmarks. [Table 4].

To examine the predictive power of toolmark properties for estimating knife blade properties and stab mechanics, four Pearson's product-moment correlations were run to assess the relationship between: 1) knife edge thickness and cut mark width, 2) floor radius and knife edge angle (sharpness), 3) serrated angle and serrate blade edge angle, and 4) knife impact trajectory and cut mark face angle [Table 5]. The results showed there was a; 1) large positive significant correlation between knife thickness and cut mark width [Fig. 15.], 2) medium significant correlation between knife edge angle and floor radius [Fig. 16.], 3) no significant correlation between serrated angle and serrate blade edge angle and 4) large positive significant correlation between cut mark face angle and knife impact trajectory [Fig. 17.].

Three preliminary linear regressions models revealed that with 95% confidence; 1) 92% of the cut mark widths could be explained by knife edge thickness, 2) 98% of the cut marks floor radii could be explained by knife edge angle and 3) 97% of the cut mark face angles could be explained by the knife impact trajectory.

310

Table. 4.

Binomial Logistic Regression values predicting likelihood of Knife type based on cut mark width, wall angle and floor radius. The model was statistically significant, $\chi2(3)=56.32$, $p<0.001$ explaining 78% (Nagelkerke R^2) of the variance in knife type and correctly classified 94% of cases. Serrated Blade Sensitivity = 94%, specificity = 94%, positive predictive value = 94% and negative predictive value = 94%.

							95% C.I. for Odds Ratio	
	B	SE	Wald	*df*	*p*	Odds Ratio	Lower	Upper
Width	4.71	1.86	6.45	1	0.011	111.5	2.935	4236
Floor radius	37.69	21.37	3.11	1	0.078	2.3×10^{16}	0.015	3.6×10^{34}
Wall angle	0.07	0.03	4.38	1	0.036	1.0	1.0	1.1
Constant	-8.08	1.98	16.63	1	0.000	0.000		

Assumptions: Linearity of the continuous variables with respect to the logit of the dependent variable was assessed via the Box-Tidwell (1962) [75] procedure. A Bonferroni correction was applied using all eight terms in the model resulting in statistical significance being accepted (Tabachnick & Fidell, 2007 [76]). Based on this assessment, all continuous independent variables were found to be linearly related to the logit of the dependent variable. There was one studentized residual with a value of 3 standard deviations, which was retained in the analysis.

311

Table 5:

Pearson's product-moment correlations and Linear Regression Models to explore the predictive power of toolmark properties for estimating knife blade properties and stab mechanics

Toolmark Property	Tool or Stab Property	Pearson correlations	Toolmark Variance explain	Prediction Equation [σ]	Linear Regression Fit	% of marks predicted at 95% confidence
Width	Knife Edge Thickness	$r(64)=0.78$, $p<0.001$ [α]	61% [μ]	Knife Edge Thickness (mm) = 0.20mm + 0.58mm * Cut Mark Width mm	$F(1,62)=96.8$, $p<0.001$	92%
Floor Radius	Knife Edge Angle	$r(64)=0.33$, $p<0.01$ [α]	11% [θ]	Knife Edge Angle (°) = 36° + 90° * Cut Mark Floor Radius°	$F(1,62)=7.5$, $p<0.01$	98%
Serrated Angle	Serrate Blade Edge Angle	$r(64)=-0.18$, $p = 0.32$ [α]	-	-	-	-
Face Angle	Knife Impact Trajectory	$r(33)=0.69$, $p<0.001$ [β]	47% [μ]	Knife Impact Trajectory (°) = 23° + 0.84° * Face Angle°	$F(1,31)=27.9$, $p<0.0005$	97%

Assumptions for two Pearson's product-moment correlations:

[α] Preliminary analyses showed that the relationships were approximately linear and had no outliers. However, with the exception of width and serrated angle, variables were not normally distributed, as assessed by Shapiro-Wilk's test. Given Pearson's correlation is relatively robust to data that is not normally distributed no corrections were performed.

[θ] Preliminary analyses showed the relationships were linear with face angle being normally distributed, as assessed by Shapiro-Wilk's test, and there were no outliers. Given that stab impact trajectories were either overhead or underarm it was unsurprising that trajectory was not normally distributed however as before no corrections were performed.

[σ] All assumptions for preliminary linear regression: Visual inspection of these two plots indicated a linear relationship between the variables and there was homoscedasticity and normality of the residuals.

[μ] Large size effect according to Cohen (1988)

[θ] Medium size effect according to Cohen (1988)

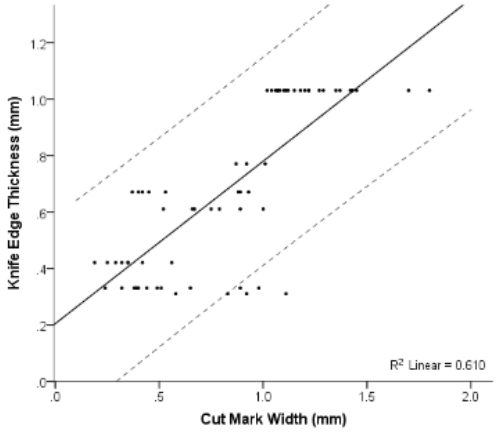

Fig. 15. *Scatterplot of Knife Edge Thickness (mm) of Knives 1-4, 6-9 used in Experiment 2, against cut mark width (mm) of cut mark created in Experiment 2. The solid line shows the linear regression fit with R^2 of 0.61 and equation y = 0.58x + 0.22. The dashed lines represent the individual confidence intervals at each prediction of the linear regression equation.*

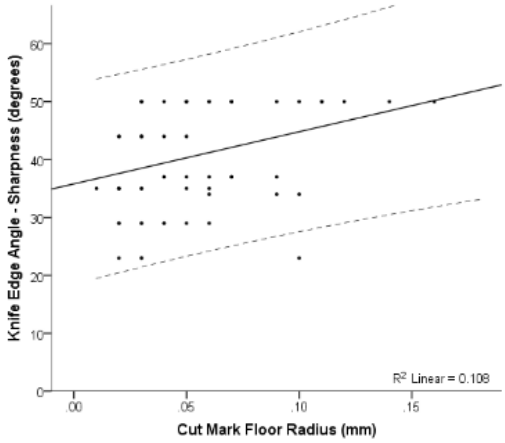

Fig. 16. *Scatterplot of Knife Edge Angle / Sharpness (degrees) of Knives 1-4, 6-9 used in Experiment 2, against cut mark floor radius (degrees) of cut mark created in Experiment 2. The solid line shows the linear regression fit with R^2 of 0.11 and equation y = 90x + 36. The dashed lines represent the individual confidence intervals at each prediction of the linear regression equation.*

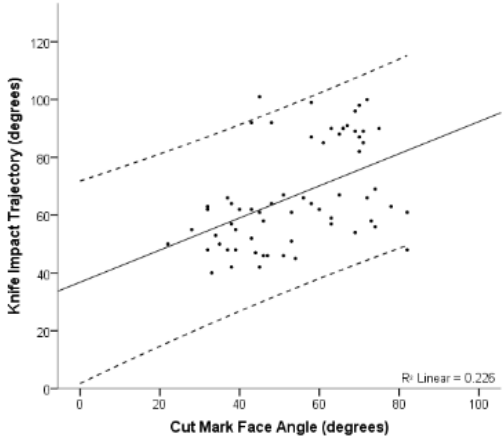

Fig. 17. *Scatterplot of Knife impact trajectory (degrees) of Knives 1-4, 6-9 used in Experiment 2, against cut mark face angle (degrees) of cut mark created in Experiment 2. The solid line shows the linear regression fit with R^2 of 0.23 and equation y = 0.84x + 23. The dashed lines represent the individual confidence intervals at each prediction of the linear regression equation.*

3.2 Knife Mark Shape Inter-rater Reliability

Three Inter-observer reliability tests for classification of cut mark shapes from micro-CT and microscope were computed. Fliess's Kappa (κ), Krippendorff's alpha (α) and average pairwise % agreement (%) were run to determine if there was agreement between the 10 trained non-forensic experts on which cut mark shape (V, T, Y, 'neither' or 'unsure') 20 pairs micro-CT and microscope cut marks were. For micro-CT images, there was good agreement between the 10 participants for all tests, (κ=0.85, p<0.005), (α=0.79, p<0.005) and (%=85, p<0.005). However, for microscope images there was poor agreement between the 10 participants for all tests (κ=0.65, p<.0005), (α=0.52, p<0.005) and (%=64, p<0.005).

3.3 Knife Mark Striations with SEM

Striations were only visible on 11 cut mark walls across 7 cut marks. Two examples (1-2) from plain non-serrated blades and two example (3-4) from serrated blades are shown below [Fig. 18.]. In line with observations of striations in the literature, striations produced by serrated blades are larger and more spaced than those from non-serrated blades which are much finer and closer together [Fig. 18.].

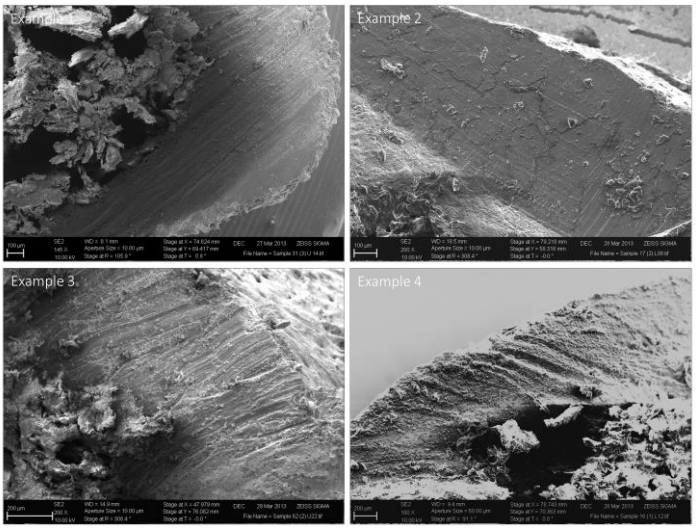

Fig. 18. *SEM images of cut mark wall striation marks from plain blades, (Example 1 from Knife 6 and Example 2 from Knife 7) and from serrated blades (Example 3 from Knife 3 and Example 4 from Knife 4)*

3.4 Model Fusion and Visualisation

Medical grade CT, micro-CT and photography were all be combined to create high resolution colour accurate 3D models that could be used for data storage facilitate data storage/processing, visualisation, 3D printing and virtual forensic exploration [Fig. 19.]. Although toolmarks were visible in the medical-CT scans, further quantitative analysis was not appropriate with this data due to the relatively low resolution.

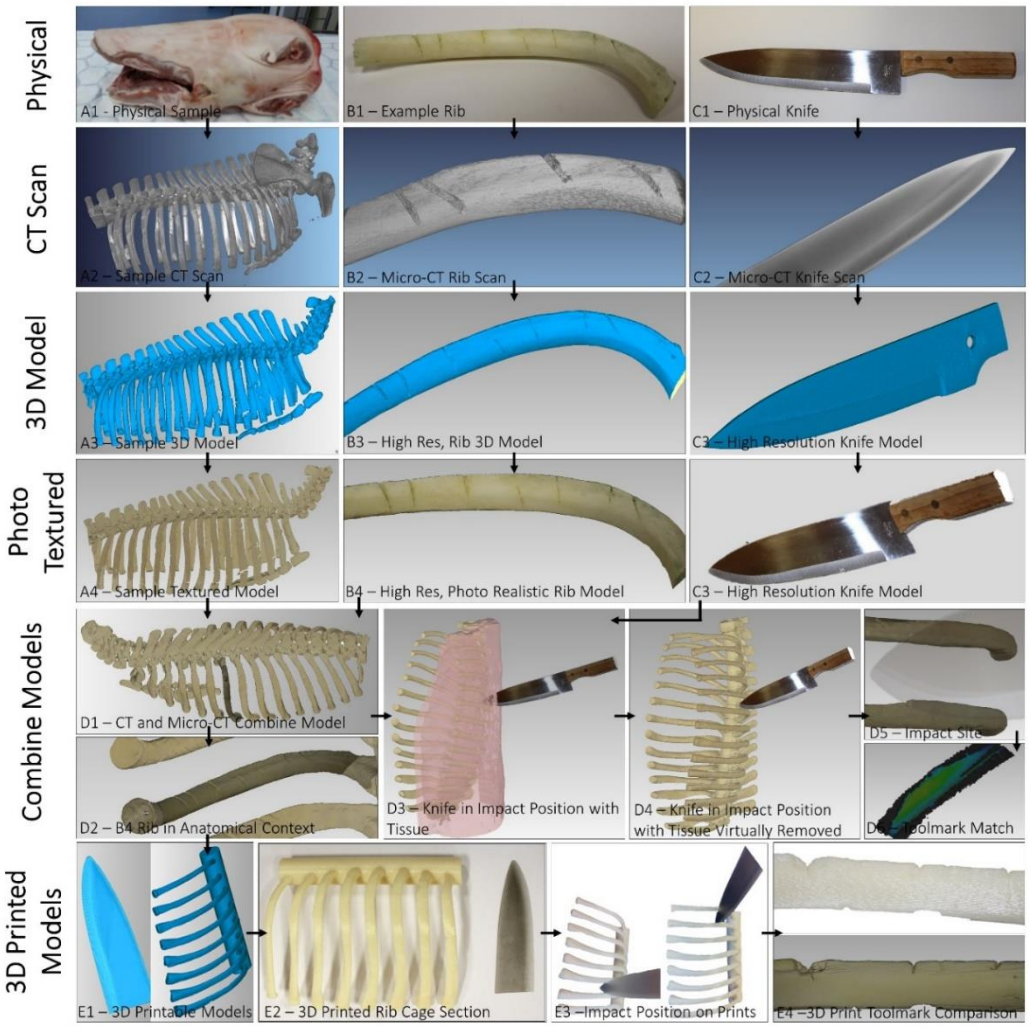

Fig. 19. *Model fusion process combining medical CT scans, micro-CT scans and digital photography for data storage, visualisation, 3D printing and virtual analysis. From the top, the pig torso [A1] which was medical CT scanned [A2] and exported as a 3D model [A3] and colour rendered [A4] providing an initial whole sample medical CT scan which included the soft and hard tissue. The micro-CT rib models could then be aligned to this anatomically accurate model. The defleshed ribs which were photographed [B1] were micro-CT scanned [B2] and exported as high-resolution 3D models [B3]. The rib photographs were then mapped onto the 3D models [B4] before the micro-CT models were aligned and fixed in anatomical position on the medical CT-based model [D1 & D2]. The physical knives [C1] were also photographed and micro-CT scanned [C2] and exported as 3D models [C3] to create photo realistic high-resolution models [C4]. These geometrically accurate knives were brought into the 3D environment with the pig torso and knife and toolmarks were matched [D3]. With the full fused model and knives, the knife trajectory could be estimated [D4] and impact site determined [D5] which can be valuable information to forensic investigators. Once knife and toolmark surfaces are aligned, surface comparison/best fit algorithms can be run to determine the percentage match. Although not the remit of this work, an example of this is shown with green indicating good surface match [D6]. Finally, a virtual section (Ribs 4-11) of the combined 3D micro-CT model was prepared for 3D printing [E1] Note that the spine was replaced by a solid cylinder for structural stability and the knife used to create the printed knife marks was also printed [E2]. The corresponding knife was printed to illustrate an example of where the knife left marks on both the underside of the rib and on the cut mark thereby allowing a physical approximation of stab trajectory to be visualised [E3]. The resolution of the 3D printer allowed for very detailed recreation of the toolmark [E4] making qualitative assessments of the knife marks possible.*

4.0. DISCUSSION

The current study had three primary aims. First, to compare toolmarks created in two contrasting experimental set ups; one highly controlled and the other a real-world simulated stabbing [Section 4.1]. Second, to evaluate and compare a range of imaging and 3D visualisation methods to identify and measure toolmark properties [Section 4.2]. Third, to statistically explore toolmark properties measured to determine whether they could be used to infer knife type or knife properties such as blade edge width [Section 4.3].

4.1. Toolmark Creation

In Experiment 1 14 cut marks were produced on dry ribs using a mechanical drop tower. This method was relatively simple, fast and allowed control of the force and location of each knife impact on the bone. It was clear that the cut marks produced by this method were very consistent in size and shape and this can be seen above [Fig. 12. & Fig. 13.]. Cut marks created by the two knife types were very distinct both qualitatively and quantitative displaying almost textbook examples of idealised V and Y shapes produced by the two blades. However, the authors suggest that extrapolating results from these idealised toolmarks is unlikely to be useful.

In Experiment 2, 64 toolmarks were generated under more real-world conditions using human agents and pig torsos. The cut marks were very different to those created in Experiment 1 where a mechanical drop rig was used. Cut marks in Experiment 2 were more variable in size and shape even when created with the same knife - this is in line with Ferllini's (2012) [23] simulated real-world study. However, this more ecologically valid method was notably more time consuming in both set up and bone extraction and resulted in substantial data attrition. Initially 320 cut marks were planned with the expectation that some of these would be lost or not be appropriate for analysis (such as cleft or puncture marks). However, knife breakages and defleshing errors resulted in a useable set of 132 cut marks across 42 ribs. After filtering out cleft and puncture marks, 64 incision cut mark were eventually micro-CT scanned with an additional 16 undergoing destructive SEM imaging. This attrition of data throughout the process demonstrates one difficulty of conducting this type of research. Nevertheless, the resulting toolmarks do allow for more ecologically valid and generalisable findings.

Care was taken in Experiment 2 to simulate as many factors relevant to real world stabbings as possible. For example, the knives sourced were representative of the typical knives carried by the public on the streets of the UK. Hunt and Cowling (1991) reported that 55% of fatal stabbings were committed using a kitchen knife and 26% with a folding knife [77]. Sharp force trauma studies typically create cut marks from 2-3 newly purchased kitchen knives which typically have fewer edge defects [23, 25-28]. The current study used knifes confiscated from the public as catalogued by the Physical Protection Group of the Metropolitan Police, UK [52]. [Fig. 3.]. The stab samples were fleshed, clothed and positioned at the average anatomical height of a male torso.

Volunteers were relatively free to stab anywhere on the sample thereby allowing natural stabbing mechanics and both overhead and underarm stab motions were used. However, the skin tension of the pig torsos as a results of multiple stabs would have likely influenced the penetrating force of the knife and therefore cut marks created later may have been different to those made at the start. Nevertheless, it is worth considering however that fatal stabbings usually involve more than one puncture of the skin. Of course, better simulation could have been achieved using human samples rather than pig although this comes with its own practical and ethical concerns and on balance, human tissue was not required for this study.

4.2. Imaging Methods

Micro-CT was an effective imaging method for capturing and visualising knife toolmarks. These observations were consistent with the previous literature and it was concluded that quantitative measures of toolmark geometry would be possible with micro-CT as demonstrated. Objective measurements of each toolmark property described [Fig. 2.] were obtained easily (e.g., typically less than 30 second per measurement) and the authors note that there was little room for interpretation error when measuring these toolmark properties. This supports previous work by Pelletti et al (2017) [10] who demonstrated high inter-rater reliability when measuring saw mark properties with micro-CT. In the present study all three inter-observer reliability tests indicate that agreement for assessing toolmark shape is more reliable when using micro-CT images compared to light microscopy. This is most likely due to the ability to create virtual cross-sections of the toolmarks using micro-CT which allows for clear 2D images of the cut mark shape. Although the observers were only given static 2D images of the toolmarks, one might suspect that being able to fully manipulate the view and cross-sections of a micro-CT scanned toolmark would further aid reliability across practitioners when judging toolmark shape. However, it should be noted that although agreement between observers was high when judging toolmark shape, it was never perfect. Unlike the toolmark shapes in Experiment 1 which were very well defined, toolmarks in Experiment 2 were much more variable making quantitative assessments more difficult. Despite micro-CT being able to improve agreement, qualitative assessment of cut mark shape is unlikely to be as effective as quantitative measures such as toolmark width. This point may deserve further exploration given the implication for forensic evidence that incorporates toolmark shape judgement.

Unlike previous imaging methods, micro-CT also allowed for the measurement of wall angle and floor radius and allowed for virtual cross sections of cut marks to be generated for shape examination. Wall angle and floor radii were found to be useful properties for distinguishing between knife type and predicting knife properties. Observing and categorising cut mark shape from micro-CT cross sections was trivial, particularly from the set of toolmarks created by the mechanical drop tower. Experiment 2 demonstrated that this was still the case when toolmarks were created under more realistic conditions and statistically tested the level of agreement between observers when assessing the cut mark shapes.

Micro-CT also allowed the creation of highly detailed 3D models for merging with other data sets. Samples in this study were defleshed before imaging to allow for other imaging methods, such as SEM and light microscopy, to take place. However, for micro-CT scanning alone this is not necessary as samples can remain intact with tissue during imaging. This can sometimes pose a challenge with physically larger samples as the distance between the emitter and detector are proportional to the spatial resolution of the scan – larger objects result in lower resolutions. The authors recommend where possible resolutions of 50µm or less to achieve optimal detail within the toolmark. Recent advances in micro-CT technology make it possible to obtain resolutions below one micronmeter as well as perform 'local zooming' with larger samples. This is particularly useful for toolmarks on long bones as significantly greater resolution can be achieved. Micro-CT scans take around 2-4 hours each depending on the scanning parameters - in the present study this equated to weeks of scanning. Studies with a greater number of toolmarks may wish to consider batch scanning multiple samples to reduce the resource required. In live forensic cases it has become clear to the authors that decisions regarding what should be scanned are crucial to allow unneccessary scans to be filtered out. Overall, given the clear benefits of micro-CT imaging in forensic cases and the growing number of facilities with this technology avalibale, the authors suggest that further toolmark studies should apply this imaging method.

We note that wall striations could not be reconstructed from the micro-CT scans most likely due to their fine structure which are smaller than the micro-CT resolutions used (10-30µm). Therefore, Scanning Electron Microscopy was used to determine the presence and diagnostic properties of wall striations for knife mark analysis. However, wall striations were only present in 44% of cut marks and rarely on both cut mark walls limiting their potential use. It is possible that fine striation marks created during knife impact were removed during the chemical defleshing process, however, given that some striation marks were clearly present, this suggestion is difficult to verify without further research. Given the small sample size, no further analysis using these striations was performed. For imaging striation marks, SEM was clearly superior to micro-CT and therefore could act as a complimentary analysis method. Imaging of striations has primarily been done in saw mark analysis where toolmarks are wider. As cut mark widths from knives are smaller SEM can only be used to image wall striations if the cut mark is separated and hence destroyed. Such destructive testing of potential evidence is often undesirable and given striation were not always visible, we support using this technique in forensic cases only as a last resort.

Initial work by Sansoni et al (2009) [36] suggested that laser scanning could be a useful tool for toolmark analysis of saw and knife marks. Findings from Experiment 1 cannot speak to the appropriateness of laser scanning for saw mark analysis, they do suggest that laser scanning is not appropriate for knife marks. Upon reviewing Sansoni et al's laser scanned knife marks figures, the authors note that the knife marks appear wide and smooth.

This larger width and smoothness was not observed in our experiment and may explain why laser scanning was much less optimal compare to previous studies. If knife mark width can sometimes pose restrictions on when laser scanning can be used optimally, the authors suggest it may be limited for knife mark analysis. Although laser scanning is clearly a useful method for other forensic applications, the authors do not recommend it for knife mark analysis as many toolmark properties will unlikely be captured.

4.3. Toolmark Analysis

This study employed a variety of statistical tests appropriate for exploring the diagnostic value of quantitative toolmark properties for the determination of knife type. To summaries: i) Knife type (serrated or plain) had a statistically significant effect of cut mark width, wall angle, floor radius and shape. ii) Knife type can be correctly estimated from cut mark width and floor radius. However, unlike cut mark width and floor radius, wall angle does not provide significant predictive power for determining knife type. iii) Knife edge thickness is highly correlated with cut mark width and this relationship can be used to estimate knife edge thickness. Floor radius however does not significantly correlate with knife edge angle (sharpness). iv) Knife impact trajectory is highly correlated with cut mark face angle and this relationship can then be used to estimate knife impact trajectory. All together this suggests that toolmark properties, when measured from micro-CT, can be a powerful forensic method for estimating knife type and properties as well as the trajectory used at knife impact.

Clearly statistical exploration of the quantitative toolmark properties obtained from micro-CT scans of the toolmarks shows promise. Cut mark width, shape, wall angle and floor radius, the latter being a new toolmark property suggested in this study, were all diagnositic properties of blade serration. In line with previous literature however, cut mark width still appears to be the most diagnositic property when investigating at the knife type level (serrated or plain) with wall angle also significantly contributing. However, as experiment 2 resulted in a small sample of cut marks per individual knife (Knife 1 = 0 marks, Knife 2 = 3 marks, Knife 3 = 7, Knife 4 = 23, Knife 6 = 8, Knife 7 = 11, Knife 8 = 8, Knife 9 = 4) it was not appropriate in the present study to statistically explore individual knife differences. This is something that will need addressing in further work that attempts to assess knife toolmark diagnosticity. Finally, the authors recommend applying the quantitative and statistical methods presented here to the analysis of micro-CT saw marks.

5.0 CONCLUSIONS

To our knowledge, this is the first study to investigate the potential of using micro-CT to facilitate quantitative statistical analysis of knife toolmarks in bone. The current study aimed to evaluate a range of toolmark analysis imaging methods and determine whether these methods can identify toolmark properties that allow for the statistical determination of knife type from toolmarks made on bone during a simulated stabbing. Although the authors consider this study to have a small sample size, it builds on initial work into quantitative toolmark analysis of knife marks with a focus on micro-CT as the imaging tool. Micro-CT is an effective 3D non-destructive method for visualizing and extracting useful toolmark properties whilst also providing additional information compared to microscopy. Micro-CT data can also be fused with other imaging methods such as medical CT or photography to generate high fidelity 3D models that allow for visualisation, 3D printing and forensic exploration. We found that inter-observer reliability when judging cut mark shape from micro-CT is good and higher than that obtained with light microscopy data suggesting that micro-CT allows for more consistent qualitative toolmark classification. Unlike micro-CT, SEM can reveal bony striation marks on the wall of knife toolmarks which can be used to infer blade serration, however in this sample, striations were not present in all of the samples. Quantitative toolmark analysis from micro-CT data can reveal statistical relationships between toolmarks and be used to estimate the knives used to create them. Specifically, knife type can be correctly determined from cut mark width and wall angle. Knife edge thickness was correlated to cut mark width and therefore cut mark width can be used to estimate knife edge thickness. Knife impact trajectory was correlated to cut mark face angle and therefore face angle can be used to estimate knife impact trajectory. Finally, knife toolmarks created by mechanical means on dry pig bones differed qualitatively from those created under more real-world conditions and therefore further toolmark analysis work is needed with more real-world conditions. Follow up studies should take quantitative approaches to toolmark analysis and we suggest micro-CT as an imaging method to facilitate this.

524 # REFERENCES

1 United Nations Office on Drugs and Crime. (2011). 2011 Global Study on Homicide: Trends, Contexts, Data (Global Study on Homicide: trends, Contexts, Data, 2011.). United Nations Office on Drugs and Crime.

2 Chaplin, R, Flatley, J and Smith, K. (2011) Findings from the British Crime Survey and police recorded crime (Second Edition) Crime in England and Wales 2010/11. London: Home Office.

3 Black, S., & Ferguson, E. (Eds.). (2016). Forensic anthropology: 2000 to 2010. CRC Press.

4 Murdock, J. J., Cavallo, J., Kreiser, J., Meyers, C., Morris, B., Sibert, B., ... & Warniment, D. (1990). Theory of identification, range of striae comparison reports and modified glossary definitions—an AFTE criteria for identification committee report. AFTE J, 22(3), 275-279.

5 Byers, S. N. Introduction to Forensic Anthropology. Third.

6 Symes, S. A. (2010). Knife and saw toolmark analysis in bone: a manual designed for the examination of criminal mutilation and dismemberment. Mercyhurst College.

7 Saville, P. A., Hainsworth, S. V., & Rutty, G. N. (2007). Cutting crime: the analysis of the "uniqueness" of saw marks on bone. International journal of legal medicine, 121(5), 349-357.

8 Marciniak, S. M. (2009). A preliminary assessment of the identification of saw marks on burned bone. Journal of forensic Sciences, 54(4), 779-785.

9 Pelletti, G., Viel, G., Fais, P., Viero, A., Visentin, S., Miotto, D., Cecchetto, G., & Giraudo, C. (2017). Micro-computed tomography of false starts produced on bone by different hand-saws. *Legal Medicine*, *26*, 1-5.

10 Pelletti, G., Cecchetto, G., Viero, A., Fais, P., Weber, M., Miotto, D., ... & Giraudo, C. (2017). Accuracy, precision and inter-rater reliability of micro-CT analysis of false starts on bones. A preliminary validation study. Legal Medicine, 29, 38-43.

11 Alunni-Perret, V., Muller-Bolla, M., Laugier, J. P., Lupi-Peégurier, L., Bertrand, M. F., Staccini, P., ... & Quatrehomme, G. (2005). Scanning electron microscopy analysis of experimental bone hacking trauma. Journal of Forensic Science, 50(4), JFS2003213-6.

12 Tucker BK, Hutchinson DL, Gilliland MFG, Charles TM, Daniel HJ, Wolfe LD. Microscopic characteristics of hacking trauma. Journal of forensic sciences. 2001;46(2):234-40.

13 Lynn KS, Fairgrieve SI. Macroscopic Analysis of Axe and Hatchet Trauma in Fleshed and Defleshed Mammalian Long Bones*. Journal of forensic sciences. 2009;54(4):786-92.

14 Thali, M. J., Taubenreuther, U., Karolczak, M., Braun, M., Brueschweiler, W., Kalender, W. A., & Dirnhofer, R. (2003). Forensic microradiology: micro-computed tomography (Micro-CT) and analysis of patterned injuries inside of bone. Journal of forensic sciences, 48(6), 1336-1342.

15 Shaw, K. P., Chung, J. H., Chung, F. C., Tseng, B. Y., Pan, C. H., Yang, K. T., & Yang, C. P. (2011). A method for studying knife tool marks on bone. Journal of forensic sciences, 56(4), 967-971.

Bolliger, S. A., Thali, M. J., Ross, S., Buck, U., Naether, S., & Vock, P. (2008). Virtual autopsy using imaging: bridging radiologic and forensic sciences. A review of the Virtopsy and similar projects. European radiology, 18(2), 273-282.

Capuani, C., Rouquette, J., Payré, B., Moscovici, J., Delisle, M. B., Telmon, N., & Guilbeau-Frugier, C. (2013). Deciphering the elusive nature of sharp bone trauma using epifluorescence macroscopy: a comparison study multiplexing classical imaging approaches. International journal of legal medicine, 127(1), 169-176.

Thompson, T. J. U., & Inglis, J. (2009). Differentiation of serrated and non-serrated blades from stab marks in bone. International journal of legal medicine, 123(2), 129-135.

Bello, S. M., & Soligo, C. (2008). A new method for the quantitative analysis of cutmark micromorphology. Journal of Archaeological Science, 35(6), 1542-1552.

Bartelink, E. J., Wiersema, J. M., & Demaree, R. S. (2001). Quantitative analysis of sharp-force trauma: an application of scanning electron microscopy in forensic anthropology. Journal of Forensic Science, 46(6), 1288-1293.

Love, J. C., Derrick, S. M., Wiersema, J. M., & Peters, C. (2012). Validation of tool mark analysis of cut costal cartilage. Journal of forensic sciences, 57(2), 306-311.

Stępień, P. (2010). Micro-geometrical characteristics of the cutting edge as the intersection of two rough surfaces. Wear, 269(3), 249-261.

Ferllini, R. (2012). Macroscopic and microscopic analysis of knife stab wounds on fleshed and clothed ribs. Journal of forensic sciences, 57(3), 683-690.

Page, M., Taylor, J., & Blenkin, M. (2011). Forensic identification science evidence since Daubert: Part II—Judicial reasoning in decisions to exclude forensic identification evidence on grounds of reliability. Journal of forensic sciences, 56(4), 913-917.

Bello, S. M., Parfitt, S. A., & Stringer, C. (2009). Quantitative micromorphological analyses of cut marks produced by ancient and modern handaxes. Journal of Archaeological Science, 36(9), 1869-1880.

Tegtmeyer, C. (2012). A comparative analysis of serrated and non-serrated sharp force trauma to bone (Doctoral dissertation).

Boschin, F., & Crezzini, J. (2012). Morphometrical analysis on cut marks using a 3D digital microscope. International Journal of Osteoarchaeology, 22(5), 549-562.

Bailey, J. A., Wang, Y., Van De Goot, F. R., & Gerretsen, R. R. (2011). Statistical analysis of kerf mark measurements in bone. Forensic science, medicine, and pathology, 7(1), 53-62.

Cerutti, E., Magli, F., Porta, D., Gibelli, D., & Cattaneo, C. (2014). Metrical assessment of cutmarks on bone: is size important?. Legal Medicine, 16(4), 208-213.

Quinn, T., & Kovalevsky, J. (2005). The development of modern metrology and its role today. Philosophical
30 Transactions of the Royal Society of London A: Mathematical, Physical and Engineering Sciences, 363(1834), 2307-2327.

Kooi, R. J., & Fairgrieve, S. I. (2013). SEM and stereomicroscopic analysis of cut marks in fresh and burned
31 bone. Journal of forensic sciences, 58(2), 452-458.

Pounder, D. J., Bhatt, S., Cormack, L., & Hunt, B. A. (2011). Tool mark striations in pig skin produced by
32 stabs from a serrated blade. The American journal of forensic medicine and pathology, 32(1), 93-95.

Pounder, D. J., & Sim, L. J. (2011). Virtual casting of stab wounds in cartilage using micro-computed
33 tomography. The American journal of forensic medicine and pathology, 32(2), 97-99.

Crowder, C., Rainwater, C. W., & Fridie, J. S. (2013). Microscopic analysis of sharp force trauma in bone
34 and cartilage: a validation study. Journal of forensic sciences, 58(5), 1119-1126.

Banasr, A., de la Grandmaison, G. L., & Durigon, M. (2003). Frequency of bone/cartilage lesions in stab and
35 incised wounds fatalities. Forensic science international, 131(2), 131-133.

Sansoni, G., Cattaneo, C., Trebeschi, M., Gibelli, D., Porta, D., & Picozzi, M. (2009). Feasibility of contactless
36 3D optical measurement for the analysis of bone and soft tissue lesions: new technologies and perspectives in forensic sciences. Journal of forensic sciences, 54(3), 540-545.

Lee, R., & Liscio, E. (2016). The accuracy of laser scanning technology on the determination of bloodstain
37 origin. Canadian Society of Forensic Science Journal, 49(1), 38-51.

Buck, U., Naether, S., Braun, M., Bolliger, S., Friederich, H., Jackowski, C., ... & Thali, M. J. (2007).
Application of 3D documentation and geometric reconstruction methods in traffic accident analysis: with
38 high resolution surface scanning, radiological MSCT/MRI scanning and real data based animation. Forensic science international, 170(1), 20-28.

Thali, M. J., Braun, M., & Dirnhofer, R. (2003). Optical 3D surface digitizing in forensic medicine: 3D
39 documentation of skin and bone injuries. Forensic science international, 137(2), 203-208.

Woźniak, K., Rzepecka-Woźniak, E., Moskała, A., Pohl, J., Latacz, K., & Dybała, B. (2012). Weapon
40 identification using antemortem computed tomography with virtual 3D and rapid prototype modeling—A report in a case of blunt force head injury. Forensic science international, 222(1), e29-e32.

Thali, M. J., Braun, M., Brueschweiler, W., & Dirnhofer, R. (2003). 'Morphological imprint': determination
41 of the injury-causing weapon from the wound morphology using forensic 3D/CAD-supported photogrammetry. Forensic science international, 132(3), 177-181.

Kettner, M., Schmidt, P., Potente, S., Ramsthaler, F., & Schrodt, M. (2011). Reverse engineering—rapid
42 prototyping of the skull in forensic trauma analysis. Journal of forensic sciences, 56(4), 1015-1017.

Ebert, L. C., Thali, M. J., & Ross, S. (2011). Getting in touch—3D printing in forensic imaging. Forensic
43 science international, 211(1), e1-e6.

Baier, W., Norman, D. G., Warnett, J. M., Payne, M., Harrison, N. P., Hunt, N. C., ... & Williams, M. A. (2017).
44 Novel application of three-dimensional technologies in a case of dismemberment. Forensic science international, 270, 139-145.

Grabherr, S., Stephan, B. A., Buck, U., Näther, S., Christe, A., Oesterhelweg, L., ... & Thali, M. J. (2007).
45 Virtopsy–radiology in forensic medicine. Imaging decisions MRI, 11(1), 2-9.

Poulsen, K., & Simonsen, J. (2007). Computed tomography as routine in connection with medico-legal
46 autopsies. Forensic science international, 171(2), 190-197.

Schnider, J., Thali, M. J., Ross, S., Oesterhelweg, L., Spendlove, D., & Bolliger, S. A. (2009). Injuries due to
47 sharp trauma detected by post-mortem multislice computed tomography (MSCT): a feasibility study. Legal medicine, 11(1), 4-9.

Rutty, G. N., Brough, A., Biggs, M. J. P., Robinson, C., Lawes, S. D. A., & Hainsworth, S. V. (2013). The role
48 of micro-computed tomography in forensic investigations. Forensic science international, 225(1), 60-66.

49 Brown, K. R. The use of μCT in forensic anthropology: identifying cause of death.

Gaudio, D., Di Giancamillo, M., Gibelli, D., Galassi, A., Cerutti, E., & Cattaneo, C. (2014). Does cone beam
50 CT actually ameliorate stab wound analysis in bone?. International journal of legal medicine, 128(1), 151-159.

Giraudo, C., Fais, P., Pelletti, G., Viero, A., Miotto, D., Boscolo-Berto, R., ... & Ferrara, S. D. (2016). Micro-
51 CT features of intermediate gunshot wounds covered by textiles. International journal of legal medicine, 130(5), 1257-1264.

Hanley, T. (2013). An Overview of MPS Knife Analyses 1995-2008. Mayor's Office for Policing and Crime:
52 Metropolitan Police - Physical Protection Group; Document Number PPG-RPT-13-002

Horsfall, I., Prosser, P. D., Watson, C. H., & Champion, S. M. (1999). An assessment of human performance
53 in stabbing. Forensic science international, 102(2), 79-89.

Annaidh, A. N., Cassidy, M., Curtis, M., Destrade, M., & Gilchrist, M. D. (2015). Toward a predictive
54 assessment of stab-penetration forces. The American journal of forensic medicine and pathology, 36(3), 162-166.

Verhoff, M. A., Ramsthaler, F., Krähahn, J., Deml, U., Gille, R. J., Grabherr, S., ... & Kreutz, K. (2008). Digital
55 forensic osteology—possibilities in cooperation with the Virtopsy® project. Forensic science international, 174(2), 152-156.

Snyder, R. G., Burdi, A., & Gaul, G. (1975). A rapid technique for preparation of human fetal and adult
56 skeletal material. Journal of Forensic Science, 20(3), 576-580.

Mann, R. W., & Berryman, H. E. (2012). A method for defleshing human remains using household
57 bleach. Journal of forensic sciences, 57(2), 440-442.

58 Fenton, T. W., Birkby, W. H., & Cornelison, J. (2003). A fast and safe non-bleaching method for forensic skeletal preparation. Journal of forensic sciences, 48(2), 274-276.

59 Motz V, Garner B, Schultz B. Defleshing of Embalmed Human Cadaveric Bone in situ. In press 2008.

60 Simonsen, K. P., Rasmussen, A. R., Mathisen, P., Petersen, H., & Borup, F. (2011). A fast preparation of skeletal materials using enzyme maceration. Journal of forensic sciences, 56(2), 480-484.

61 Luther, P. G. (1949). Enzymatic maceration of skeletons. In Proceedings of the Linnean Society of London (Vol. 161, No. 146).

62 Mairs, S., Swift, B., & Rutty, G. N. (2004). Detergent: an alternative approach to traditional bone cleaning methods for forensic practice. The American journal of forensic medicine and pathology, 25(4), 276-284.

63 Gram, C.O., (2006) Vertebrate Skeletons: Preparation and Storage: National Park Service

64 Boyle, C. (2010). Maceration and Preparation of Mammal Skeletons for Long-Term Curation. Archaeology and forensic laboratory. University of Indianapolis.

65 Haydon, H. L., & Green, H. (1934). A rapid method of preparing clean bone specimens from fresh or fixed meterial. The Anatomical Record, 61(1), 1-4.

66 Thornby, J., Landheer, D., Williams, T., Barnes-Warden, J., Fenne, P., Norman, D., ... & Williams, M. A. (2014). Inconsistency in 9mm bullets: Correlation of jacket thickness to post-impact geometry measured with non-destructive X-ray computed tomography. Forensic science international, 234, 111-119.

67 Sim, J., & Wright, C. C. (2005). The kappa statistic in reliability studies: use, interpretation, and sample size requirements. Physical therapy, 85(3), 257-268.

68 Viera, A. J., & Garrett, J. M. (2005). Understanding interobserver agreement: the kappa statistic. Fam Med, 37(5), 360-363.

69 Carletta, J. (1996). Assessing agreement on classification tasks: the kappa statistic. Computational linguistics, 22(2), 249-254.

70 Cohen, J. (1960). A coefficient of agreement for nominal scales. Educational and psychological measurement, 20(1), 37-46.

71 Hunt, R. J. (1986). Percent agreement, Pearson's correlation, and kappa as measures of inter-examiner reliability. Journal of Dental Research, 65(2), 128-130.

72 Fleiss, J. L. (1971). Measuring nominal scale agreement among many raters. Psychological bulletin, 76(5), 378.

73 Norman, D. G., Getgood, A., Thornby, J., Bird, J., Turley, G. A., Spalding, T., & Williams, M. A. (2014). Quantitative topographic anatomy of the femoral ACL footprint: a micro-CT analysis. Medical & biological engineering & computing, 52(11), 985-995.

Norman, D., Metcalfe, A. J., Barlow, T., Hutchinson, C. E., Thompson, P. J., Spalding, T. J., & Williams, M. A.
74 (2017). Cortical bony thickening of the lateral intercondylar wall: the functional attachment of the anterior cruciate ligament. The American journal of sports medicine, 45(2), 394-402.

Box, G. E., & Tidwell, P. W. (1962). Transformation of the independent variables. Technometrics, 4(4), 531-
75 550.

76 Tabachnick, B. G., Fidell, L. S., & Osterlind, S. J. (2001). Using multivariate statistics.

77 Hunt, A. C., & Cowling, R. J. (1991). Murder by stabbing. Forensic science international, 52(1), 107-112.

525